Advantages of BARC and photoresist matching for 193-nm photosensitive BARC applications

Joyce Lowes[a], Victor Pham[b], Jim Meador[a], Charlyn Stroud[a], Ferdinand Rosas[b], Ramil-Marcelo L. Mercado[a], Mark Slezak[b]
[a]Brewer Science, Inc., 2401 Brewer Drive, Rolla, MO 65401, USA
[b]JSR Micro, Inc., 1280 North Mathilda Avenue, Sunnyvale, CA, 94089, USA

ABSTRACT

As the semiconductor industry approaches smaller and smaller features, applications that previously used top anti-reflective coatings have now begun using developer-soluble bottom anti-reflective coatings (BARCs). However, there are several drawbacks to a wholly developer-soluble system, mainly because many of these systems exhibit isotropic development, which makes through-pitch and topography performance unsatisfactory. To solve this problem, we have developed several photosensitive BARC (PS BARC) systems that achieve anisotropic development. One issue with the PS BARC, as with traditional dry BARCs, is resist compatibility. This effect is compounded with the photosensitive nature of our materials. The acid diffusion and quenching nature of the resists has been shown to have a significant effect on the performance of the acid-sensitive PS BARC. Some resists contain a highly diffusive acid that travels to the PS BARC during the post-exposure bake and aids in clearance. Others show the opposite effect, and the same PS BARC formulation is not able to clear completely. To address the lack of compatibility and to further improve the PS BARC, we have developed a solution that properly matches PS BARC and photoresist performance.

Keywords: Photosensitive BARC, ArF, photoresist, developer-soluble, anisotropic development, topography

1. INTRODUCTION

As the integrated circuit (IC) industry realizes the importance of using developer-soluble BARCs[1], the demand for more advanced materials increases exponentially. Several approaches[2] have been attempted to achieve good performance with these materials, but thus far, two main divisions of developer-soluble BARCs have emerged. The first iteration of developer-soluble BARCs were designed to develop away in standard photoresist developer. These materials develop isotropically, and performance is highly dependent on develop rate, leaving concerns of undercutting of the lithographic profile. For implant applications, differences in topography will lead to thickness differences of the coated developer-soluble BARC film. If the thickness change and develop rate of this type of developer-soluble BARC is not precisely managed, failure of the lines can occur simultaneously with incomplete clearance of the developer-soluble BARC. To solve these issues, a second type of developer-soluble BARC was developed. This type of BARC, a PS BARC, was modeled after chemically amplified photoresists and develops anisotropically. Behavior in developer is not controlled by develop rate, rather by exposure dose.

During early development, PS BARCs were designed and tested as independent layers. Once a successful layer was found that met optical and photosensitivity requirements, it would be screened with a variety of photoresists. If needed, further optimization of the PS BARC formulations was done independent of photoresists. Further complicating issues is the migration of photogenerated acid from the photoresist film into the PS BARC film. The PS BARC had to be tuned for one photoresist. Once a new photoresist was selected, the components may have behaved differently, requiring this process to begin anew. While this worked for early generations of PS BARCs at relaxed critical dimensions (CDs)[3], as implant layer resolution requirements were reduced and advanced implant photoresists were designed, this independent method of development was not sufficient to meet industry demand. To achieve maximum PS BARC and photoresist performance, the PS BARC behavior was tuned to work well with a particular category of implant photoresists. Initially, PS BARC formulations were modified with various photoacid generators (PAGs) and quenchers that offered similar chemical behavior as the photoresist's PAGs and quenchers. Optimization of lithographic performance was

J. Lowes, V. Pham, J. Meador, C. Stroud, F. Rosas, R.-M.L. Mercado, M. Slezak, "Advantages of BARC and photoresist matching for 193-nm photosensitive BARC applications," *Proceedings of SPIE*, vol. 7639, 2010, in press.

accompanied by other factors such as residue and developer sensitivity. The resulting system gave good dark field/bright field and iso/dense performance with little mask biasing and common depth of focus (DOF).

While this approach resulted in acceptable performance for the 32-nm node, further improvements were needed for decreased residue, post-exposure bake (PEB) sensitivity, and better resolution to prepare for future nodes. The next path of development was to design the PS BARC polymer platform to behave more similarly to the photoresist polymer via matching of the deprotection mechanism and solubility properties. PS BARC platforms were designed with various acid-labile protecting groups. The various polymer platforms were formulated and tested for desired BARC properties such as solvent resistance, optics at 193 nm, basic contrast behavior, and post-develop residue (PDR). Lithography was also performed with several photoresists of varying activation energies.

2. EXPERIMENTAL

2.1 Chemistry

PS BARC formulations were designed with a polymer containing carboxylic acid moieties combined with a multifunctional crosslinker, photoacid generator (PAG), quencher, and industry-acceptable solvents. JSR Micro, Inc., supplied the ArF photoresists used in this study.

2.2 Film properties

To determine solvent resistance, PS BARC formulations were spin coated onto 4-inch silicon wafers and then baked on a hot plate at 160°C for 60 seconds. Ethyl lactate solvent was puddled on the wafer for 20 seconds, and then spun dry. Film thickness was measured before and after processing. A J.A. Woollam Co. M-2000® variable-angle spectroscopic ellipsometer (VASE) was used to determine the optical constants n and k at 193 nm. Contrast curve measurements were performed using 200-mm wafers coated via a Clean Track ACT® 8 and baked at 160°C for 60 seconds. Wafers were exposed via open-frame exposure on a 193-nm scanner. Various post-exposure bakes (PEBs) ranging from 100°-120°C were performed and then the wafers were developed in 0.26N aqueous tetramethylammonium hydroxide (TMAH) for 45 seconds then rinsed with deionized (DI) water and spun dry. In some cases, JSR photoresist was applied atop the PS BARC layer.

2.3 PROLITH modeling

PROLITH version 10.1 from KLA-Tencor was used for all thickness simulations.

2.4 Post-develop residue determination

PDR was measured using wafers generated from the contrast curve measurements. Native oxide thickness of the substrate was measured before coating using a M-2000® VASE. Once the wafer was coated, the M-2000® VASE was used to determine the Cauchy coefficients of the PS BARC film. After exposure and development, the areas within the individual exposed die were measured again via the M-2000® VASE. Using the native oxide, Cauchy coefficients, and final thickness, a model was built on the M-2000® VASE to calculate the average thickness of any remaining PDR.

2.5 Lithography

All lithographic performance was done using a 193-nm scanner. PS BARC thickness was optimized at 55 nm and JSR photoresist at 195 nm. PS BARC bake was 160°C for 60 seconds. The post-application bake (PAB) for the JSR photoresist was 110°C for 60 seconds. PEB was done at various temperatures ranging from 100°-120°C for 60 seconds, then the wafers were developed in 0.26N TMAH for 45 seconds, rinsed in DI water, and spun dry. Top-down CD profiles were measured using a Hitachi S9380. Cross-sections were performed using Hitachi S-4300 cross-section SEM. Exposures were done using a TEL Clean Track™ ACT 8 and Nikon S305B scanner (NA=0.68, 0.6 sigma) using conventional illumination.

3. RESULTS AND DISCUSSION

3.1 Initial formulation screening

Initial formulation design was performed with a PS BARC polymer and multifunctional crosslinker that showed promising performance with several JSR photoresists at 150 nm and larger CDs. However, the PAG and quencher that

were traditionally added to this PS BARC formulation displayed dissimilar chemical behavior and performance to those incorporated into the JSR photoresist. As a result, this original formulation did not perform well at CDs smaller than 140 nm. Initially, to study the effect of PAG and quencher on litho performance, three formulations were made with various loadings of PAG and quencher, as shown in Table 1. Polymer and crosslinker loadings were kept constant in the PS BARC formulation. The first formulation (A) without PAG and quencher was added to study the diffusion rate of the photoresist-generated acid into the PS BARC film. A second formulation (B) included quencher to study the effectiveness of quencher incorporation into the PS BARC film. Lastly, PAG and quencher were added to another formulation (C).

Table 1. Table showing PAG and quencher loadings in the experimental formulations.

Formulation	PAG loading	Quencher loading
A	none	none
B	none	standard
C	low	standard

The n and k at 193 nm were 1.67 and 0.55, respectively. These numbers were modeled using PROLITH software to find the best thickness, as shown in Figure 1. First-minimum thickness of the PS BARC was 38 nm, however, for adequate coverage and performance over topography[4], the first-maximum thickness was selected at 55 nm.

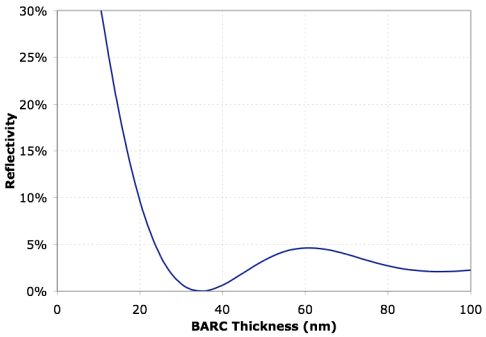

Figure 1. Reflectivity curve on silicon for ArF PS BARC formulation.

These three PS BARC formulations were screened with JSR JSR-ARF1 resist for bright field (BF) and dark field (DF) feature performance. Results are shown in Figure 2. At 140 nm, 1:2 DF features, the sample without PAG and without quencher does not have adequate diffusion of acid from the resist to sufficiently clear the PS BARC. In the BF features, the PS BARC does begin to clear in the open areas, however, there is still a significant amount of PS BARC remaining at the base of the lines. When quencher is added to the system, the PS BARC system behaves as expected, and the acid is kept from diffusing completely into the open areas of the PS BARC film, causing increased scumming. With PAG incorporated, there is still a small amount of residue in the DF feature, however, the BF features show clean profiles and minimal footing. In the isolated line, undercutting of the PS BARC profile is observed, indicating the need to modify the amount of quencher and, conversely, the amount of PAG in the system.

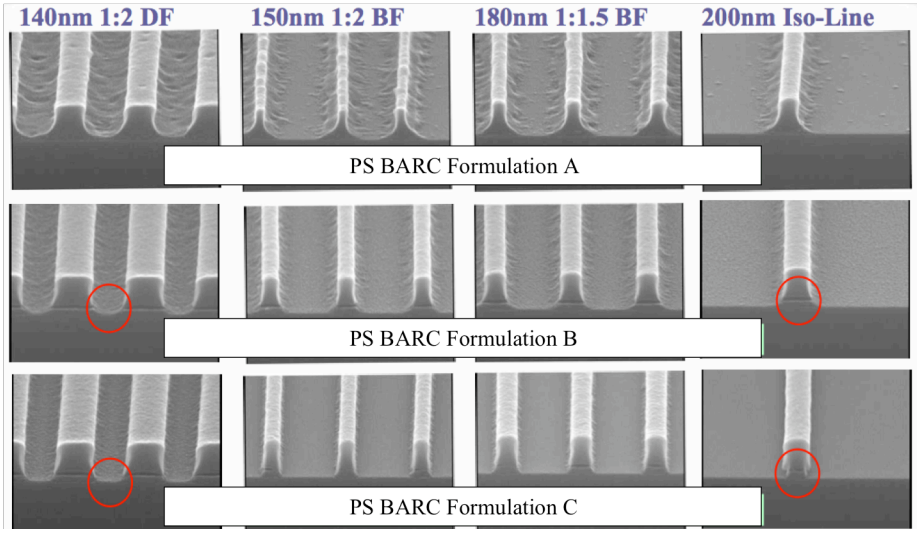

Figure 2. Lithographic profiles of formulations A, B, and C with JSR-ARF1 resist.

3.2 Initial formulation optimization

Once promising performance was found with the initial round of formulation screening, new PAG and quencher components were selected that closely matched the photogenerated acid and quencher characteristics of that of the JSR photoresist. Again, polymer and crosslinker loadings were kept constant, while a low and medium level of PAG and quencher were screened. Results for these two formulations are shown in Figure 3.

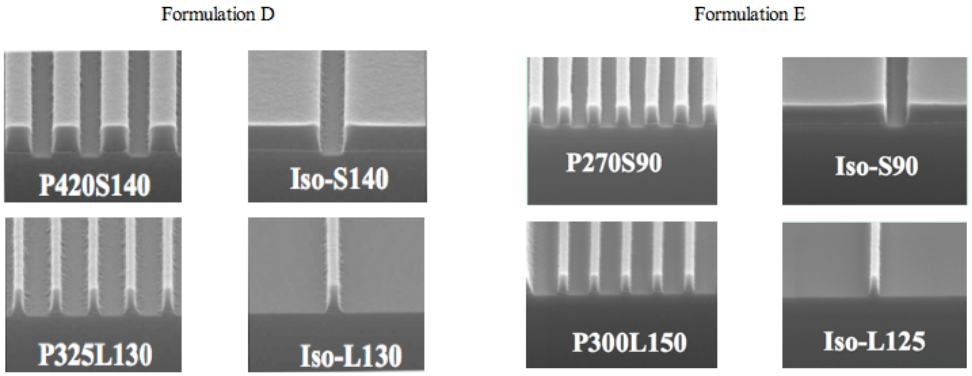

Figure 3. Lithographic performance of optimization formulations D (low PAG) and E (medium PAG).

The first formulation (D) shows good CD performance between the DF and BF features. No mask biasing is needed to achieve the isolated line at the same dose that resolves the dense DF features. The lines are clean with only a small amount of footing. Formulation E shows a similar DF/BF bias with much better resolution and profile shape and very little footing at the base of the lines. These results show that with only two iterations of formulation screening, and by matching the components and behavior of the PS BARC and photoresist, we were able to modify a PS BARC/photoresist combination that performed much better than modifying the PS BARC alone.

3.3 Polymer modification

While formulation E performed well lithographically at 130-nm CDs, this system exhibited a few issues. Although this platform is able to resolve some features smaller than 130 nm, the process window and common depth of focus (DOF) suffered. The mode of failure for resolution is lack of imageability of the PS BARC. At the dose to size for the photoresist, the PS BARC is not able to image properly and the result is massive footing. Additionally, on some substrates, this platform leaves behind a layer of PDR that may pose an issue for some critical implant layers.

Expanding on the idea of making the PS BARC more like a photoresist and improving the resolution and residue issues, it was determined that improvements to the polymer were needed.

The initial PS BARC polymer contained three components, a carboxylic acid moiety for crosslinking, a chromophore, and acid-labile protected base-soluble group. For the standard polymer, the crosslinking site controls the majority of the function of the PS BARC, while the protecting group only functions minimally. In the current system, the leaving group does not efficiently deprotect at the PEBs used. In a photoresist, the protecting group controls most of the photoresist's ability to be soluble. As new, better-resolution photoresists are developed, monomers with lower activation energy (E_a) are incorporated to help improve contrast. With this understanding of photoresist development, the PS BARC polymer was modified. New acid-labile groups were investigated to study their effect on resolution capability and residue. From previous studies, changing the acid-labile group of the PS BARC also improves the amount of PDR[5] remaining after PS BARC exposure and development. Three protecting groups were selected that more closely matched the E_a of advanced ArF photoresists, shown in Figure 4. Isopropyl adamantyl methacrylate (IpAdMA) and ethyl adamantyl methacrylate (EAdMA) were chosen because they show improved contrast in ArF photoresists[6].

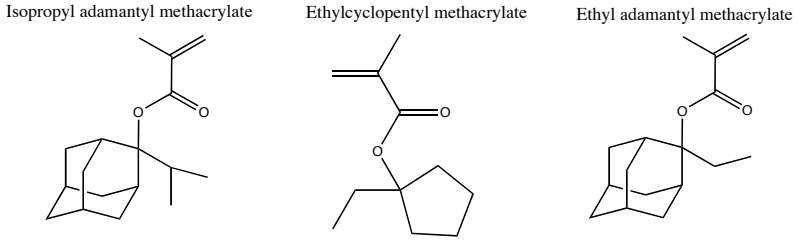

Figure 4. Various protecting-group monomers used in the study.

A series of polymers based on the original PS BARC polymer platform were synthesized by replacing the standard protecting group with the monomers listed in Figure 4. To keep the optical properties identical to the original PS BARC platform, the chromophore level was kept constant for all polymers. Other factors, such as molecular weight and polydispersity, were also kept similar to the original. Polymers were formulated using equal crosslinker, PAG, and quencher loadings as in PS BARC formulation E. Solvent resistance was tested using ethyl lactate to ensure the PS BARC crosslinked properly. For all new polymer systems, stripping in ethyl lactate was less than 0.5%, indicating proper crosslinking of the PS BARC. Contrast curves of the PS BARC films were then tested, and compared to formulation E. The data, in Figure 5, show that by incorporating the monomers with lower E_a, the slope of the contrast curve is much sharper than that of the standard PS BARC, mimicking the behavior of photoresist. By increasing the PAG loading, contrast can be further improved.

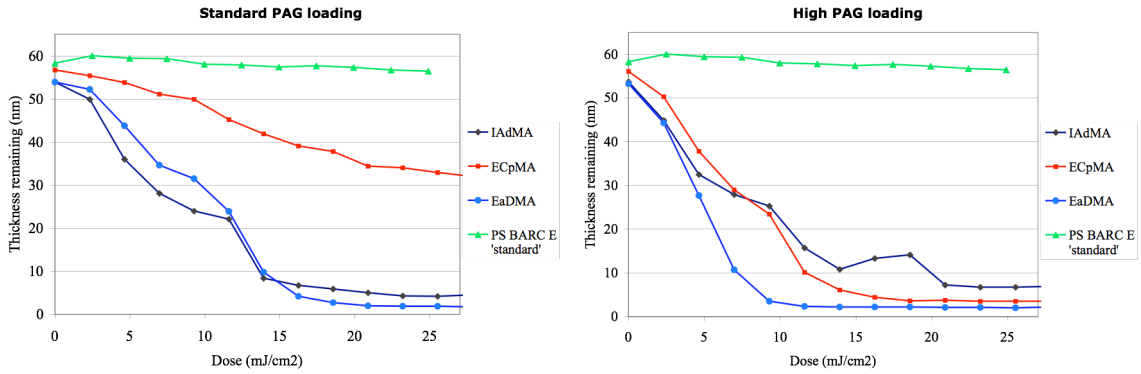

Figure 5. Contrast curve of PS BARC formulations made using monomers with lower E_a at 110°C PEB. Increasing PAG loading sharpens the contrast even further.

3.4 Photoresist PAG study

As shown in Figure 5, the PS BARC does not clear completely without contribution from the photoresist. This type of behavior has been observed before and can be attributed to acid diffusion from the photoresist[5,7]. The effect of the

photoresist's PAG was studied by testing PAGs of various molecular weights. Table 2 shows the details for the PAGs used in this study.

Table 2. Description of PAGs used.

Photoresist	Relative PAG size
A	Small
B	Large
C	Small and Large

Photoresist A contains a relatively small PAG. Photoresist B contains a large, bulky PAG that could have difficulty traveling through the film, therefore diffusion may be limited. Photoresist C contains a mixture of the small and the bulky PAGs. The IpAdMA BARC formulation was used for this study. A photoresist polymer having medium E_a was used and molar concentrations of PAGs kept constant. Lithographic results for BF and DF features are shown in Figure 6. The high mobility of the small PAG allows it to diffuse into the PS BARC and aid in the decrosslinking and deprotection of the film. The bulky PAG is able to properly clear the photoresist, but without the added acid, the PS BARC is not sufficiently cleared. When a mixture of the two PAGs is used, the PS BARC clears somewhat better, but the concentration of small PAG is not enough to completely clear the film.

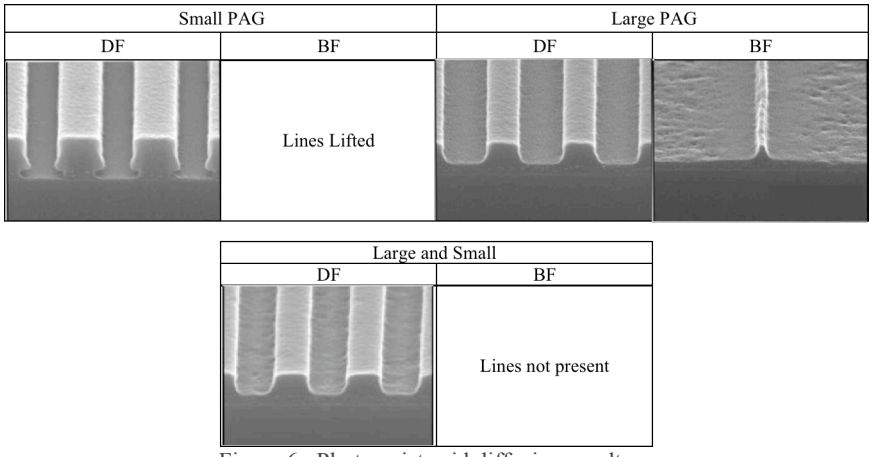

Figure 6. Photoresist acid diffusion results.

3.5 Lithographic screening

To study the effect of these PS BARCs having lower E_a on lithographic capability, three JSR photoresists were selected which are used at different E_a levels. The three JSR photoresists are listed in Table 3 along with the relative E_a of each of the platforms.

Table 3. JSR photoresists used and the relative activation energy of each.

Photoresist	**Relative activation energy (Ea)**
JSR-ARF1	Low
ARX3001JN	Medium
JSR-ARF2	High

Each new PS BARC formulation was tested at standard and high PAG loadings. To investigate the amount of PAG diffusion from the photoresist into the PS BARC, each polymer was also formulated without PAG and quencher.

The standard and high PAG samples were tested with the photoresist having relatively high E_a, JSR-ARF2 resist. For all three of the new PS BARC platforms, this resist was a poor match. Overall, at the dose and PEB required to properly image this photoresist, the PS BARC was beginning to be overexposed, resulting in undercut and line collapse. With the IpAdMA PS BARC, regardless of PAG loading, at the dose where the photoresist will typically start printing, the lines are completely gone. These results indicate that the E_a of the IpAdMA is much too low for this high-E_a photoresist. The

EAdMA behaves similarly, and, based on similar contrast curves from Figure 5, this might be expected. Next, the ECpMA PS BARC formulation shows slightly better performance with JSR-ARF2 resist. From the contrast curve, this platform had the highest dose requirements and, therefore, may be able to withstand the dose required to image this photoresist. At the standard PAG loading, in underexposed areas, only the dense and semi-dense standing lines were present and the isolated line was collapsed. However, as the dose increased to be closer to the proper dose to size, the semi-dense and then dense lines began to collapse. For both the EAdMA and ECpMA platforms, as the PAG loading decreased, the lines were collapsing at a lower dose. To study the effect of PAG loading, further testing was done with the EAdMA- and ECpMA-based platforms that contain no PAG. For both platforms, lines could be printed, but the PS BARC film did not clear completely, indicating the need for PAG.

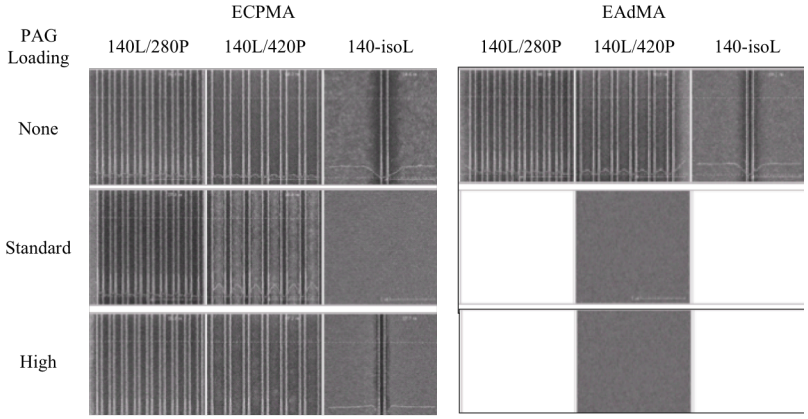

Figure 7. Litho performance of the new PS BARC platforms with JSR-ARF2 resist.

Evaluation with the photoresists having medium and low E_a, ARX3001JN resist and JSR-ARF1 resist, respectively, was performed next. A PAG-less sample of each new platform was added to investigate how much the photoresist acid contributes to the PS BARC clearance. For ARX3001JN resist, for all the PAG loadings tested, the IpAdMA platform resulted in complete collapse of all lines before the photoresist was able to resolve. With the EAdMA testing with ARX3001JN resist, at the lowest dose, lines remain, but, as with the IpAdMA, massive line collapse occurred far before dose to size for the photoresist. The ECpMA platform, as with the higher-E_a photoresist, performs better with ARX3001JN resist. At the standard and high PAG loadings, this PS BARC showed standing dense, semi-dense, and isolated lines with a large exposure margin. Coincidently, the PAG-less sample showed some line collapse, perhaps indicating that a modification is needed to counteract the effect of acid diffusion from the photoresist.

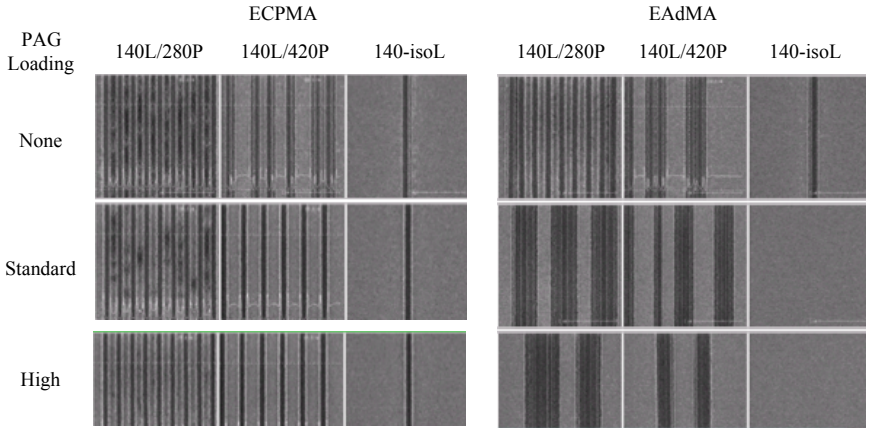

Figure 8. Litho performance of the new PS BARC platforms with ARX3001JN.

IpAdMA performance with JSR-ARF1 resist showed incomplete clearance in the non-PAG sample. In the standard and high PAG loadings, the lines were collapsing. Again, the ECpMA and IpAdMA both performed better than the IpAdMA. For ECpMA, the non-PAG sample performed well. At the higher PAG conditions, line collapse occurred only at very high doses. The EAdMA performs almost as well, with good performance and slight residue at the non-

PAG loading. At the standard PAG loading, the residue was reduced with line collapse at very high doses. However, increasing PAG further resulted in line collapse at low doses.

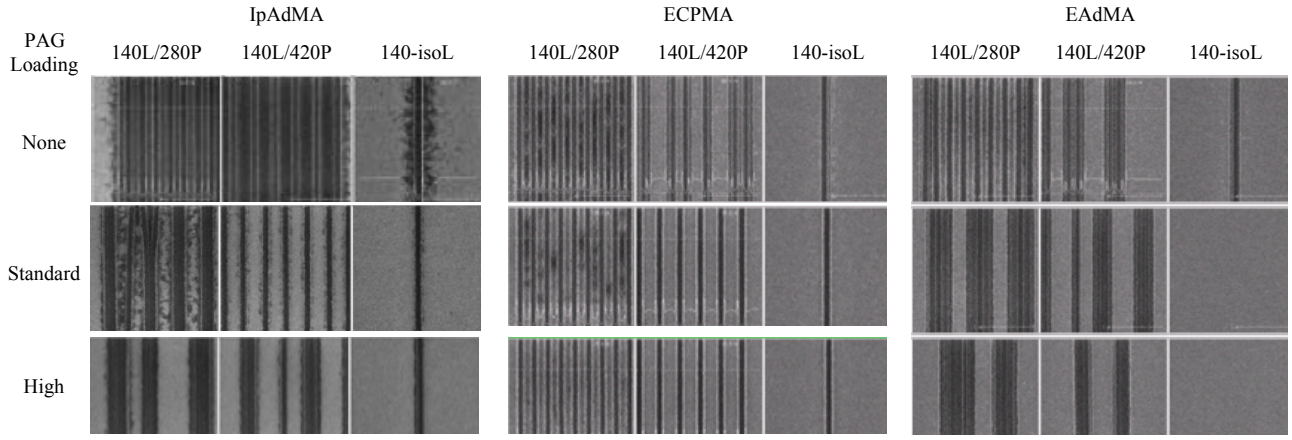

Figure 9. Litho performance of the new PS BARC platforms with JSR-ARF1 resist.

Overall, incorporating the lowest E_a monomer, IpAdMA, into a photoresist-type PS BARC did not produce the desired results. While this monomer works well in other standard PS BARCs[5], it was not a good match for this study. The ECpMA and EAdMA both gave promising results, therefore, we continued testing these two platforms.

3.6 Post-develop residue testing

Once two platforms that gave acceptable litho performance had been found, our next selection criterion was the amount of PDR produced. From the lithographic study, ARX3001JN resist performed the best, so the PDR test was performed with this resist coated on the PS BARC. Each of the ECpMA and EAdMA platforms were tested at the standard and high PAG loadings and then compared to the standard PS BARC E. Figure 10a shows the contrast curve data, and Figure 10b shows the PDR values across dose, relative to the standard PS BARC E.

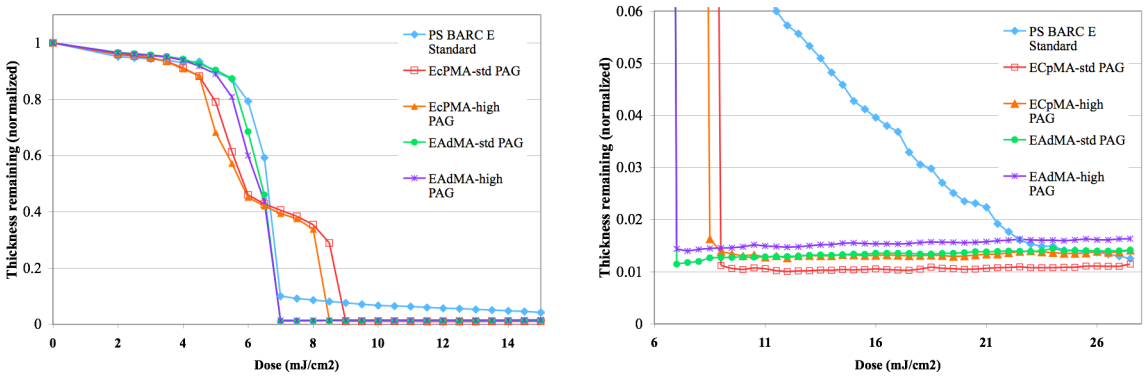

Figures 10a and 10b. On the left, Figure 10a shows the contrast curve measurements for all formulations tested. On the right, Figure 10b shows the PDR values, relative to the standard PS BARC E.

As previously shown in the contrast curves from the PS BARC films alone (Figure 5), both of these platforms produce much less residue than the standard PS BARC E. From Figure 10b, the ECpMA PS BARCs produce the overall lowest PDR, closely followed by the EAdMA. PDR values at 20 mJ/cm^2 were compared for all formulations, as shown in Table 4. As the PAG loading increases, the amount of PDR does not decrease. Rather, the PDR is slightly higher. As the PAG amount in these formulations is increased, the quencher loading is equimolar to the PAG loading, thus negating any potential effects of increased acid in the film. The ECpMA gives the lowest amount of PDR at either PAG loading, at an average of 50 percent less PDR than the standard.

Table 4. PDR values for the new PS BARC platforms at 20 mJ/cm^2.

Platform	PAG level	PDR (normalized)	% change from standard
Standard	Standard	1.0	-
ECpMA	Standard	0.44	56 %
ECpMA	High	0.55	45 %
EAdMA	Standard	0.58	42 %
EAdMA	High	0.66	34 %

Analysis of the PDR data and comparison of initial lithographic performance allow us to select the ECpMA platform as a good match to the medium-E_a photoresist. While the EAdMA platform also performs well, in order to develop a solution more quickly, we focused on only one platform.

3.7 Photoresist modification

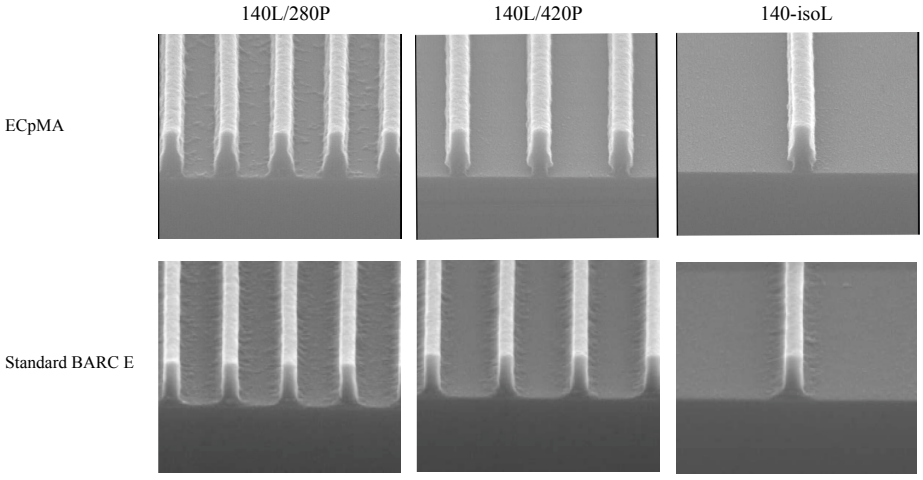

Figure 11. Cross-section results of ECpMA PS BARC and standard PS BARC E with ARX3001JN resist.

Figure 11 shows the cross-section profiles of the ECpMA formulation with the high PAG loading with ARX3001JN compared to PS BARC E with the same photoresist. Even though the amount of residue produced improved over the standard PS BARC, we wanted to study how modifications to the photoresist formulation affect performance of the PS BARC. For this initial study, to keep from introducing too many new variables in performance, the polymer and PAG chemistries were kept constant. Using ARX3001JN resist, derivatives were made varying quencher type and loading. In the first set of photoresist formulations, the PS BARC quencher was substituted in place of the standard photoresist quencher. When the PS BARC quencher was added into the photoresist formulation, there was no measurable difference between the two, which showed that there were no quencher compatibility issues between the PS BARC and photoresist, but no beneficial effect was derived. Next, we wanted to investigate the effect of saturating the system with excess quencher. By increasing the amount of quencher, the dose requirement for the photoresist should increase, and with that excess exposure, the PS BARC will be exposed to more light, without overexposing the photoresist. This excess light should generate more acid in the PS DBARC, aiding in lower PDR. Keeping the PS BARC formulation constant, the standard photoresist quencher was increased by 33% and 67%. Lithographic and PDR testing was done for both experimental photoresists. The sample having 67% more quencher exhibited excess scumming across all tested conditions. For the sample having 33% more quencher, lithographic profiles were similar to those for the standard ARX3001JN resist, albeit at a higher dose. Qualitatively, visible residue is also reduced with this combination.

3.8 Further PS DBARC/photoresist modification

Once accurate matching of the resist and PS DBARC has been recognized, further modification was done to both systems to further align them. A PS DBARC polymer was made using ECpMA in the polymer. As in the original screening, three different resists, with various E_a polymers were used. Resist details are shown in Table 5. Typical PEBs required for these polymers are also listed. Both PS DBARC and resist were made using the same PAG and same quencher. The PS BARC was screened at one PAG loading with all three resists.

Table 5. New JSR resists used and the relative activation energy of each.

Photoresist	Relative activation energy (E_a)	Standard PEB
JSR-ARF3	Low	120°C
SUN6119	Medium	100°C
JSR-ARF4	High	110°C

With the lowest E_a resist, this new PS BARC formulation clears completely, but severely undercuts the resist. When paired with the high E_a resist, the PS BARC performs well in the bright field features, but the dark field features do not clear completely. As with the previous studies, the medium E_a resist gives the best results with this PS BARC formulation. Bright field features are standing through pitch and dark field features have better clearance than the low E_a resist.

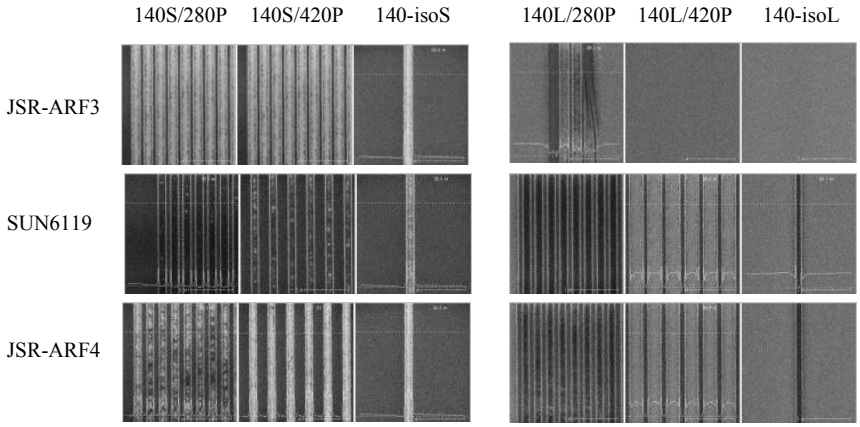

Figure 12. Top-down results for new PS BARC and resist screening.

With promising results from the medium E_a resist, PEB changes were done to determine if better clearance could be obtained in the dark field areas. Lithography was tested from 100°C to 120°C. Only an increase of 5°C is required to completely clear the dark field features. At the PEBs higher than 110°C, the bright field features begin to collapse. Figure 13 compares lithographic profiles for 100°C and 105°C PEBs. At 105°C, the profiles are straight with minimal residue and undercut.

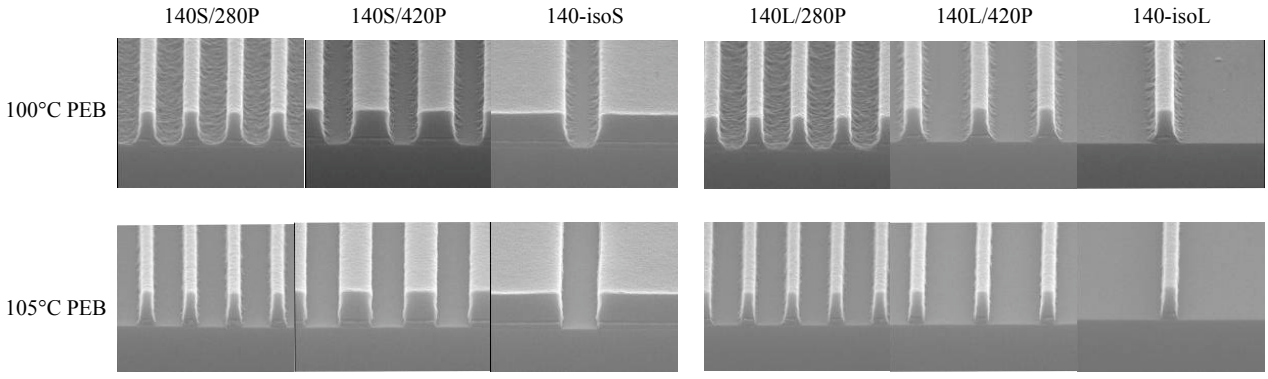

Figure 13. Lithographic profiles through pitch for 100°C and 105°C with medium E_a photoresist and new PS BARC.

4. CONCLUSIONS

Previous attempts at modifying PS BARCs resulted in acceptable performance, but improvements were incremental and slow. We have also learned that the photosensitive nature of our materials causes the photoresist to have a large effect on PS BARC performance. Down to a certain resolution, the PS BARC and photoresist can be made to work independently of each other. However, when resolution reaches the requirements for the 32-nm node and beyond, independent photoresist/PS BARC modification will not suffice. PAGs and quenchers closely matching those in the photoresist were first added into the PS BARC. While this gave acceptable performance, further improvements were needed, so the PS BARC polymer was modified to more closely match the photoresist and then evaluated against various photoresist chemistries. The results show that by matching the PS BARC chemistry along with modifying the photoresist, we have developed a method that decreases product design time while improving performance.

REFERENCES

[1] Lee, H.-R., Popova, I. Y., Rolick, J. M., Gomez, J.-M., and Bailey, T. C., "Message to the undecided – Using DUV dBARC for 32 nm node implants," *Proc. SPIE* 7273, 72730Y (2009).

[2] Mercado, R.-M. L., Lowes, J. A., Washburn, C. A., and Guerrero, D. J., "A novel approach to developer-soluble anti-reflective coatings for 248-nm lithography," *Proc. SPIE* 6519, 65192X-1 – 65192X-10 (2007).

[3] Meador, J., Beaman, C., Lowes, J., Washburn, C., Mercado, R., Nagatkina, M., and Stroud, C., "Development of 193-nm wet BARCs for implant applications," *Proc. SPIE* 6153, 854-863 (2006).

[4] Washburn, C., Guerrero, A., Mercado, R., Guerrero, D., and Meador, J., "Process Development for Developer-Soluble Bottom Anti-Reflective Coatings (BARCs)," *INTERFACE 2006: Proceedings of the 43rd Microlithography Symposium*, (2006).

[5] Meador, J. D., Lowes, J. A., Stroud, C., Thomas, S., Qiu, Y., Mercado, R.-M. L., Pham, V. and Slezak, M., "Improving the performance of light-sensitive developer-soluble anti-reflective coatings by using adamantly terpolymers," *Proc. SPIE* 7273, 727312-1 – 727312-9 (2009).

[6] Kazuya, F., Tanaka, S., Matsumoto, N., Ohna, H., Kawano, N., Yamane, H., Hatakeyama, N., and Ito, K., "Leading-edge adamantly polymers designed for 193 nm lithography," *Proc. SPIE* 6923, 692335-1 – 692335-9 (2008).

[7] Guerrero, D. J., Mercado, R., Washburn, C., and Meador, J., "Photochemical Studies on Bottom Anti-Reflective Coatings," *Journal of Photopolymer Science and Technology* 19(3), 343-347 (2006).